AD-A101 426   NAVAL RESEARCH LAB   WASHINGTON DC   F/G 20/7
                STABILITY CONSIDERATIONS FOR LIGHT-ION BEAM TRANSPORT IN Z-DISC--ETC(U)
                JUL 81   P F OTTINGER, D MOSHER, S A GOLDSTEIN
UNCLASSIFIED   NRL-MR-4548   NL

END
DATE
FILMED
11-81
DTIC

REPORT DOCUMENTATION PAGE	READ INSTRUCTIONS BEFORE COMPLETING FORM

1. REPORT NUMBER	2. GOVT ACCESSION NO.	3. RECIPIENT'S CATALOG NUMBER
NRL Memorandum Report 4548	AD-A102 426	

4. TITLE (and Subtitle)	5. TYPE OF REPORT & PERIOD COVERED
STABILITY CONSIDERATIONS FOR LIGHT-ION BEAM TRANSPORT IN Z-DISCHARGE CHANNELS	Interim report on a continuing NRL problem
	6. PERFORMING ORG. REPORT NUMBER

7. AUTHOR(s)	8. CONTRACT OR GRANT NUMBER(s)
P.F. Ottinger,* D. Mosher and S.A. Goldstein*	

9. PERFORMING ORGANIZATION NAME AND ADDRESS	10. PROGRAM ELEMENT, PROJECT, TASK AREA & WORK UNIT NUMBERS
Naval Research Laboratory Washington, D.C. 20375	Sponsor Assignment No. DE-A108-79DP40092 NRL Prob 47-0879-0-1

11. CONTROLLING OFFICE NAME AND ADDRESS	12. REPORT DATE
Department of Energy Washington, D.C. 20545	July 8, 1981
	13. NUMBER OF PAGES
	25

14. MONITORING AGENCY NAME & ADDRESS(If different from Controlling Office)	15. SECURITY CLASS. (of this report)
NRL-MR-4548	UNCLASSIFIED
	15a. DECLASSIFICATION/DOWNGRADING SCHEDULE

16. DISTRIBUTION STATEMENT (of this Report)

Approved for public release; distribution unlimited.

17. DISTRIBUTION STATEMENT (of the abstract entered in Block 20, if different from Report)

18. SUPPLEMENTARY NOTES

*Present address: Jaycor, Inc., Alexandria, VA 22304

19. KEY WORDS (Continue on reverse side if necessary and identify by block number)

intense ion beams
transport
instabilities
z-discharge channels

20. ABSTRACT (Continue on reverse side if necessary and identify by block number)

Light-ion beams, appropriate for use as inertial-confinement fusion drivers, can be transported in z-discharge channels over distances of several meters. Here stability considerations for light-ion beam transport in such channels are reviewed. Many aspects of the important velocity-space instabilities are considered and the resulting conditions for good transport are discussed. The results will be presented in a general form so that they may be applied to beams of various species (e.g. H_0^+, D_t^+, C^{+4}, etc.) propagating in channel plasmas of different composition (e.g. hydrogen, argon, air, etc.).

DD $_{1 \text{ JAN } 73}^{\text{FORM}}$ 1473   EDITION OF 1 NOV 65 IS OBSOLETE
S/N 0102-014-6601

CONTENTS

iii

STABILITY CONSIDERATIONS FOR LIGHT-ION BEAM
TRANSPORT IN Z-DISCHARGE CHANNELS

1. INTRODUCTION

The development of terawatt-level ion beams has generated a great deal
of interest in using light-ion beams to drive thermonuclear pellets.[1-9]
Target design studies for light-ion beams indicate that $\sim$ 2 MJ of ions must
be delivered in $\sim$ 10 nsec to an $\sim$ 1 cm diameter pellet in order to achieve
high-gain thermonuclear ignition.[10] Since present technology can provide up
to 5 TW single-generator modules from which up to 200 kJ of ions can be
extracted in $\sim$ 50 nsec, a multimodule system is required. In addition, a
transport scheme and a method for beam pulse compression are needed.

One possible transport scheme involves the use of a z-discharge channel
for transporting a prefocused ion beam (Fig. 1).[11] Focusing is achieved by
a combination of geometric and magnetic-field focusing prior to injection into
the channel.[12,13] Beam pulse compression results from ramping the diode
voltage such that the tail of the beam catches up to the front of the
beam.[13,14] The ideal diode voltage waveform is $\phi(t) = \phi_o(1-t/t_a)^{-2}$ for
$0 \le t \le \tau_b < t_a$ where τ_b is the beam pulse duration and t_a is the beam arrival
time at the target.

Assuming that the z-discharge channel is produced in a MHD stable con-
figuration, the question of the effects that the passage of the beam will have
on the equilibrium and stability of the beam-plasma system is an important
one. The MHD response of the plasma has been treated elsewhere[15] and will
only be briefly reviewed here. Analysis of stable beam propagation in
straight and tapered channels, as well as in bumpy channels (subject to
sausage instability) has also been done previously.[16] This work shows that,
in the absence of microinstabilities driven by the beam, good beam transport
and bunching is possible under the conditions set by MHD considerations
(which will be outlined in Sec. 2). However, in the presence of microinsta-
bilities, beam transport and bunching can be seriously affected.

Analysis of electrostatic (ES)[17] and electromagnetic (EM)[18] velocity-
space instabilities, which can grow on a time scale much faster than the beam
pulse duration, will be reviewed in this report. The problem will be con-
sidered with the goal of identifying the conditions for good transport and
bunching. The results will be presented in a general form so that they may
be applied to beams of various low atomic number species propagating in
channel plasmas of different compositions.

2. BEAM-PLASMA SYSTEM IN THE TRANSPORT CHANNEL

The beam-plasma system consists of a focused ion beam propagating down the axis of an externally-driven z-discharge plasma channel.[13,19] The ion beam is focused at the entrance to the plasma channel (see Figs. 1 and 2) with velocity components transverse to z given by $V_\perp/V_z = \tan \alpha \ll 1$. The current being driven in the preformed z-discharge channel provides the radial confinement of the beam. Because of the small perpendicular beam energy, the channel current can be much less than the beam current. A high plasma density in the channel insures good beam charge neutralization.[20] Good beam current neutralization in the interior of the beam also occurs, so that the total magnetic field is comparable to that associated with the preformed channel established before beam injection. Because $J_p = J_{ch} - J_b \approx -J_b$, the electron drift velocity is approximated by $V_e \approx n_b Z_b V_b / Z_p n_p$, where n_b and n_p are the beam and plasma ion densities, Z_b and Z_p are the beam and plasma ion charge states, and J_p, J_b and J_{ch} are the plasma, beam and preformed channel current densities, respectively. Note that the electron density is $Z_p n_p$.

Hydrodynamic modeling of the background plasma[15] shows that a uniform net-current model is appropriate for the early times associated with passage of the beam front. This is because the low-temperature channel is established microseconds before beam injection so that complete magnetic diffusion occurs. Later in the ion pulse, $J_p \times B$ expansion of the beam-heated high-temperature plasma reduces the magnetic field strength in the interior of the channel. The built-up field in the expanding cylindrical shock wave is also enhanced by significant current non-neutralization in the cool plasma surrounding the beam-heated channel. The maximum field strength just outside the ion-beam radius can exceed that established by the preformed z-discharge current by a large factor. Thus, at late times during beam passage, the magnetic field distribution can be approximated by a surface-current model. Although the induced $V_r \times B_\theta$ electric field is important when considering beam energy losses during transport, at no time does the electric field become large enough to significantly affect the stability analysis.

The linearized stability analysis presented here strictly applies only when the mode under consideration grows on a time scale faster than any changes in the beam-plasma system (i.e., $\gamma > \tau_b^{-1}$). For growth on a time scale slower than the beam pulse duration, the perturbation analysis breaks down since small perturbations will be washed out by the zero-order changes in the system before growth can occur. Thus for those modes which are shown to e-fold less than once during the passage of the beam, the results should be interpreted as showing that significant growth does not occur.

The distribution of particles in axial velocity is illustrated in Fig. 3. The plasma ions form a stationary background while the drift of the plasma electrons provides for beam current neutralization. Because of the high plasma density, this drift velocity, V_e, does not exceed the electron thermal velocity even before the beam heats the plasma. As the beam passes through a given point, the plasma is heated and the conductivity increases. The electron-ion collision frequency, ν_{ei}, decreases but the electrons generally remain collisional ($\nu_{ei} > \omega_{ce}$) at all times during the pulse for purposes of the stability analysis. Since the electron-ion equilibration time is on the order of the beam pulse duration the electron temperature will not exceed the ion temperature by more than a factor of ten.

The ion beam density is typically much less than the plasma density and, beams of interest are nonrelativistic. The spread in axial velocities, designated by V_t in Fig. 3, is on the order of $V_b \alpha_m^2/2$ before beam bunching occurs. Here V_b is the beam velocity and α_m is the maximum ion injection angle into the channel. For $\alpha_m = 0.1-0.2$ rad, V_t/V_b is relatively small. As the beam bunches, V_t/V_b can increase by an order of magnitude as the faster ions generated later in the pulse catch up to slower ions at the front of the beam. The beam pulse duration, τ_b, decreases and the beam density, n_b, increases as the beam bunches. The dependence of the beam parameters on axial position due to bunching will be expressed explicitly as $V_t(z)$, $\tau_b(z)$, etc.

Since the ES stability analysis depends strongly on the shape of the beam distribution function, it is important to use a theoretical model which contains the appropriate physics. For a distribution in v_z which has a large slope on the low velocity side such as illustrated in Fig. 4a, a resistive instability persists in spite of the thermal spread in v_z and the high frequency of collisions between the plasma electrons and ions.[21,22] However, if the slope of the distribution function is not as sharp, such as for the Gaussian distribution shown in Fig. 4b, electron-ion collision are damping if the thermal spread in v_z is sufficiently large. The slope of the distribution function on the high velocity side does not affect the stability analysis.

Before the beam bunches, the distribution in v_z is determined by the injection condition. Since the ions are injected into the channel nearly uniformly over a range of angles predominately in the r-z plane and since the time-averaged axial velocity for an ion injected at a given α varies like $V_t(1-\alpha^2/2)$, the distribution in v_z rises slowly as indicated in Fig. 4c. Additional smoothing out of the distribution in v_z will result from beam energy spreading due to radial variations in the diode voltage. The stability properties of this distribution closely resemble those of the Gaussian distribution. The beam ion distribution after bunching is also similar in shape to Fig. 4c. Since the ion diodes which are used in the experiments have a constant impedance behavior during the duration of the ion pulse, more ions (higher currents) are generated at higher energies as the diode voltage ramps upward. Thus in the bunched state there are more ions at higher velocities than at lower velocities and the spread in axial velocities is on the order of $(2Z_d e/m_i)^{1/2}(\phi_f^{1/2}-\phi_0^{1/2})$. Here Z_d is the charge state of the beam ions in the diode and ϕ_0 and ϕ_f are the initial and final diode voltages. This spread can be considerably larger than the initial spread before bunching $(V_t \sim V_b \alpha_m^2/2)$.

Thus a Gaussian distribution can be used to properly model the ion beam distribution function both before and after bunching when considering ES modes. When the analysis is not sensitive to the detailed shape of the distribution function (e.g. for analyzing the stability of EM modes), simpler models may be used.

3. LINEAR STABILITY ANALYSIS

The results of linear stability analyses reported previously[17,18,22] are presented here in a more general form so that they may be applied to beams of various species. The composition of the channel plasma is also unspecified. Growth rates will vary as the beam heats the channel plasma and as the channel expands. The changes in the hydrodynamic structures of

3

the channel occur gradually over the pulse duration of the beam. Growth rate
expressions appropriate near both the front and the tail of the beam are
presented in order to determine how hydrodynamic changes alter the results.
Most notably these changes include (1) a reduction in the e-i collision
frequency at the tail of the beam where the plasma is heated, and (2) a reduc-
tion in the magnetic field in the interior of the channel at late times in the
pulse as the now highly conducting heated plasma expands due to $\underline{J} \times \underline{B}$ forces.
Near the front of the beam, the beam ions follow betatron-like orbits while
at the tail of the beam, the beam ions move in more straight line-like orbits
with reflections off of the magnetic field piled up at the edge of the
channel.

3.1. ES Modes

The ES modes are the fastest growing modes when driven unstable.
Unstable growth will generally reach nonlinear saturation on a time scale much
faster than the beam pulse duration. These modes involve either charge
bunching (e-b and e-i modes) or density bunching (ion-acoustic mode) and
generally exhibit their largest growth for $\underline{k} = k\hat{e}_z$, which is a result of the
small thermal spread in the axial direction before axial beam compression
occurs.

3.1a. e-b Two Stream Mode

The e-b two stream instability is driven by the relative streaming
between the beam ions and plasma electrons. In general the beam can be
considered warm because $V_t(z)/V_b \gtrsim 2[m_e z_b^2 n_b(z)/m_b Z_p n_p]^{1/3}$ even before beam
bunching occurs. Here m_b is the beam ion mass. Near the front of the beam
the betatron motion of the ions can reduce the growth rate of the mode which
is given by

$$\gamma_1 = -\frac{\nu_{ei}}{2} + 0.76 \frac{\omega_{pb}^2(z)}{\omega_{pe}} \left(\frac{V_b}{V_t(z)}\right)^2 R \tag{1}$$

where $\omega_{pb}^2 = 4\pi e^2 z_b^2 n_b(z)/m_b$ and $\omega_{pe}^2 = 4\pi e^2 Z_p n_p/m_e$ are the beam and electron
plasma frequencies respectively. The electron-ion collision frequency is
given by $\nu_{ei} = 1.45 \times 10^{-6} z_p^2 n_p \lambda_{ei}/T_e^{3/2}$, where T_e is in eV and λ_{ei} is the
Coulomb logarithm. The reduction factor, R, equals the fraction of beam ions
which can effectively participate in the wave growth. If $\gamma_1 > 2\omega_\beta$, which is
the usual case, all ions can participate and R = 1. Here $\omega_\beta = (V_b \omega_{cb}/r_c)^{\frac{1}{2}}$ is
the ion betatron frequency and ω_{cb} is the beam cyclotron frequency. If
$\gamma_1 \lesssim 2\omega_\beta$, only those ions with $\Delta z < 1/k$ can participate, where Δz is the
amplitude of the betatron oscillations about $z = \bar{v}_z t$ (see Fig. 5). The
amplitude, Δz, depends on the ion injection conditions, $r(z=0)$ and $\alpha(z=0)$.[17]
If this amplitude is large, the ion moves across many wave fronts before the
instability e-folds even once, and thus cannot effectively participate in
wave growth. The value of R must be calculated from the actual distribution
function. For a Gaussian distribution $R \sim 8\omega_\beta V_b/kV_t^2$ for $k > 8\omega_\beta V_b/V_t^2$ and
$R = 1$ for $k < 8\omega_\beta V_b/V_t^2$. At the tail of the beam, betatron effects are less
important, so that R = 1 in Eq. (1).

4

Beam heating of the plasma can considerably reduce the damping term in Eq. (1) as e-i collisions become less frequent. Beam bunching, on the other hand, reduces the driving term in Eq. (1) as V_t increases dramatically. Thus the potentially most dangerous position for wave growth lies at the tail of the beam (R = 1) at the beginning of the transport channel before significant beam bunching occurs.

3.1b. e-i Two Stream Mode

The e-i two stream mode is driven by the relative streaming between the background electrons and ions. The electrons drift with an average velocity $V_e \sim n_b Z_b V_b / Z_p n_p$ relative to the stationary ions and in general $V_e < u_e$. Here u_e is the thermal velocity of the electrons. The expression for the growth (damping) rate is

$$\gamma = -\nu_{ei} - (\pi/8)^{\frac{1}{2}} \frac{kc_s}{(1+k^2\lambda_{De}^2)^2} \left\{ Z_p (T_e/T_i)^{3/2} \exp\left[- \frac{T_e}{2T_i(1-k^2\lambda_{De}^2)}\right] \right.$$

$$\left. + \frac{m_e}{m_i}\left(1 - \frac{V_e}{c_s}\left[1+k^2\lambda_{De}^2\right]^{\frac{1}{2}}\right)\right\} \tag{2}$$

where $c_s = (T_e/m_i)^{\frac{1}{2}}$ is the ion sound speed, $\lambda_{De} = (T_e/4\pi e^2 Z_p n_p)^{\frac{1}{2}}$ is the electron Debeye length and where a simple Krook model was used for the collision term. In deriving Eq. (2), it was assumed that $\nu_{ei} < kc_s/(1+k^2\lambda_{De}^2)^{\frac{1}{2}}$. When $T_e \sim T_i$ this reduces to

$$\gamma_2 \approx -\nu_{ei} + (\pi/8)^{\frac{1}{2}} \frac{kc_s}{(1+k^2\lambda_{De}^2)^{3/2}} \left\{ \frac{V_e}{u_e} - \frac{Z_p \exp\left[-\frac{1}{2(1+k^2\lambda_{De}^2)}\right]}{(1+k^2\lambda_{De}^2)^{\frac{1}{2}}} \right\} . \tag{3}$$

Since V_e is usually less than u_e, the mode is typically stable.

3.1c. Ion-Acoustic Mode

If $T_e \gg T_i$, then the drifting electrons can drive an ion-acoustic instability. In this case Eq. (2) reduces to

$$\gamma_3 \approx -\nu_{ei} + \left(\frac{\pi m_e}{8m_i}\right)^{\frac{1}{2}} \frac{k}{(1+k^2\lambda_{De}^2)^{3/2}} \left[V_e - \frac{c_s}{(1+k^2\lambda_{De}^2)^{\frac{1}{2}}}\right] \tag{4}$$

This predicts instability ($\gamma > 0$), if $V_e/c_s > (1+k^2\lambda_{De}^2)^{-\frac{1}{2}}$ and if ν_{ei} is sufficiently small. However, the severity of the condition on T_e/T_i is often overlooked. For V_e/c_s as large as 5, T_e/T_i must be greater than 12 for instability even for $k\lambda_{De} \ll 1$. Figure 6 shows the critical values of T_e/T_i for instability versus k for various values of V_e/c_s (assuming $\nu_{ei} = 0$). Since T_e/T_i is not expected to reach such high levels, in general ion-acoustic turbulence is not expected.

3.1d. ES Stability Conditions

Since the e-b mode is the only ES instability which could be generated, it is important to state under which conditions it may be avoided. For stability ($\gamma_1 \leq 0$) Eq. (1) states that

$$\frac{z_p^{5/2} n_p^{3/2} \lambda_{ei}}{T_e^{3/2}} \geq 3.2 \times 10^7 \frac{z_b^2 n_b(z) V_b^2}{\mu_b V_t^2(z)} \qquad (5)$$

is required. Here $\mu_b = m_b/m_H$, T_e is measured in eV and all other variables are in Gaussian units. This condition used in conjunction with the condition

$$n_p \approx 1.4 \times 10^{12} \, I_{ch} r_{ch}^{-2} \, (I_b(z) \tau_b(z)/S)^{\frac{1}{2}} \quad , \qquad (6)$$

derived from MHD considerations[15], set constraints on n_p and T_e for good transport. Here I_{ch} and I_b are measured in amps and S is the beam stopping power of the plasma measured in $erg \cdot cm^2/g$. Eq. (6) gives the ion density in the channel required for minimum beam energy loss in the channel during transport. Given this required ion density, Eq. (5) sets an upper limit on T_e, beyond which electrostatic turbulence will set in. For good transport both of these conditions must be satisfied. Generally the stability criterion in Eq. (5), is most severely tested at the tail of the beam where T_e is largest and at the beginning of the transport channel before significant bunching occurs where $V_t(z)$ is smallest ($V_t(z)/V_b \sim \alpha_m^2/2$).

3.2 EM Modes

The EM modes are slower growing modes than the ES modes, so that even if the mode is unstable, growth may not have sufficient time to reach non-linear saturation during the pulse duration of the beam. The modes are nearly purely growing (i.e. do not convect with the beam) and involve current bunching or filamentation of the beam and/or plasma channel. The wave vector, $\underset{\sim}{k}$, is oriented perpendicular to the direction of beam propagation with $\underset{\sim}{k} = k\hat{e}_r$ for the Weibel mode (radial current bunching) and $\underset{\sim}{k} = k\hat{e}_\theta$ for the whistler mode (azimuthal current bunching). In addition, the cylindrical geometry dictates that $k_r \gtrsim 2\pi/r_b$ and $k_\theta \gtrsim \ell/r_b$ where ℓ is an integer.

3.2a. Beam-Whistler Mode

The beam-whistler instability is driven unstable by the relative streaming motion between the beam ions and the channel plasma. Since the wave vector is in the azimuthal direction and the beam ions execute their betatron orbits in the r-z plane, the betatron motion of the beam has little effect on the mode. However, a small spread in angular momentum, which is observed experimentally, can reduce the growth rate significantly. With no spread in angular momentum ($V_\theta^2/c^2 < 2\nu_{ei}\omega_{pb}V_b/c\omega_{pe}^2$) the growth rate is

$$\gamma = \omega_{pb}(z) V_b/c \quad , \qquad (7)$$

6

and with $v_\theta^2/c^2 > 2\nu_{ei}\omega_{pb}(z)V_b/c\omega_{pe}^2$ the peak growth rate is

$$\gamma_4 = 2\nu_{ei}\omega_{pb}^2(z)V_b^2/V_\theta^2\omega_{pe}^2 \qquad (8)$$

at $k \sim \gamma_4/V_b$. Here V_θ is a measure of the thermal spread in the azimuthal velocity of the beam ions. If $kr_b < 1$, peak growth rate is reduced to $[1-(k_o r_b)^{-2}]\gamma_4$ because of geometry constraints and if $k_o r_b < 1$, no growth is possible. The critical wavenumber $k_o = \sqrt{2}\omega_{pb}(z)V_b/cV_\theta$ [see Eq. (35), Ref. 18].

If there is wave growth at a given point in z, the number of e-folds that occurs is just

$$N = \int_0^{\tau_b(z)} \gamma(t)dt , \qquad (9)$$

where the time dependence of the plasma parameters must be considered. Most importantly ν_{ei} decreases at $T_e^{-3/2}(t)$ as the plasma is heated by the passing beam. Note that beam thermal effects do not completely quench the instability because of the finite plasma resistivity. Given information from MHD considerations on the time variation of the plasma parameters due to beam passage, one can then determine from Eq. (9) whether significant azimuthal beam current bunching occurs.

3.2b. Beam-Weibel Mode

For the beam-Weibel instability the wave vector is in the radial direction. In this case the spread in perpendicular velocities associated with the betatron motion of the beam ions reduces the growth rate of the instability. A measure of the radial velocity spread is given by $V_o\alpha_m$, so that the peak growth rate is given by

$$\gamma_5 = 2^{4/5}\nu_{ei}\omega_{pb}^2(z)/\omega_{pe}^2\alpha_m^{8/5} \qquad (10)$$

at $k \sim \gamma_5/V_b\alpha_m^{7/5}$. Again the number of e-folds that occur at a given point in z can be determined by Eq. (9) and MHD considerations. Since the thermal spread in the radial velocity is typically comparable or larger than the thermal spread in the azimuthal velocity, the beam-Weibel instability is generally less dangerous than the beam-whistler mode. A superposition of both unstable modes, however, will lead to beam filamentation.

3.2c. Plasma-Electron Mode

If beam thermal effects or geometry constraints prevent the beam from driving strong EM wave growth, instability can still result from the electron return current established with the plasma. Because of the high collisionality ($\nu_{ei} > \omega_{ce}$) of the plasma electrons, radial ($\underline{k} = k\hat{e}_r$) and azimuthal ($\underline{k} = k\hat{e}_\theta$) EM modes driven by the plasma electrons are essentially indistinguishable (aside from small geometric effects). The analysis must include electron thermal effects, as well as collisional effects since the

7

electron streaming velocity is subthermal even early in the pulse before beam heating occurs.

At early times in the pulse when $\omega_{pe}u_e/c\nu_{ei} > 1$, the peak growth rate is

$$\gamma = (\omega_{pi}V_e/c)(2-z_p^{-1})^{\frac{1}{2}} \quad . \tag{11}$$

Later in the pulse after the beam heats the plasma if $\omega_{pe}u_e/c\nu_{ei} > 1$, then thermal effects slows the growth of the mode. The maximum growth rate is then given by

$$\gamma = 2^{-3/2}\omega_{pe}V_e^2/cu_e \quad . \tag{12}$$

At all times in the pulse geometry constraints prevent wave growth if $k_o r_b < 1$ where in this case $k_o = \omega_{pe}V_e/\sqrt{2}u_ec$. Since again this mode does not convect, the number of e-folds at a given point in z can be obtained from Eqs. (11), (12) and (9) and MHD considerations.

3.2d. EM Stability Conditions

If the growth rates of the EM instabilities are slow enough such that less than one e-fold (N<1) occurs during beam passage, wave growth will be washed out by the MHD changes in the beam-plasma system. Only wave growth with N>1 will affect beam transport. In order to prevent the beam from filamenting, the beam should then have

$$\alpha_m^2 \geq V_\theta^2/V_b^2 > 1.6\times10^{-9}\,\frac{n_b(z)}{\mu_b}\int_0^{\tau_b(z)}\left(\frac{z_p\lambda_{ei}}{T_e^{3/2}}\right)dt \quad , \tag{13}$$

where again T_e is in eV's and n_b is measured in cm^{-3}. This condition is derived from Eq. (8) for azimuthal current bunching which is typically more severe than the condition for radial current bunching since α_m is usually greater than V_θ/V_b. Here it is also assumed that $\sqrt{2}\omega_{pb}(Z)r_bV_b/cV_\theta > 1$, which is the usual case. In order to evaluate Eq. (13), a knowledge of the MHD response to beam passage is required, in particular, one must know the time history of the electron temperature.

If the beam is warm enough to prevent beam filamentation (i.e., Eq. (13) is satisfied), it is still possible for the channel to filament. Channel filamentation is avoided if

$$\frac{J_b(z)}{n_p^{\frac{1}{2}}}\left(\frac{9.4\times10^1}{\mu_p^{\frac{1}{2}}}\int_0^{t_1(z)}(2-z_p^{-1})dt + 6.9\times10^4\,J_b(z)\int_{t_1(z)}^{\tau_b(z)}\frac{dt}{n_p z_p^{3/2}T_e^{\frac{1}{2}}}\right) \leq 1 \quad . \tag{14}$$

Here $\mu_p = m_p/m_H$, $J_b(z) = z_b e n_b(z) V_b$, J_b is measured in sA/cm^2 and t_1 is defined as the time it takes for the beam to heat the plasma

to $T_e^1 = 1.4\times10^{-4}(z_p^3 t_1 n_p \lambda_{ei}^2)^{1/4}$ in eV. If $T_e(0) > T_e^1$, then $t_1 = 0$ and the first term in Eq. (14) does not contribute. If $t_1 \gtrsim \tau_b$, then the second term in Eq. (14) does not contribute and the limits on the integration of the first term go from 0 to $\tau_b(z)$. In Eq. (14) it was assumed the $\omega_{pe} r_b V_e / 2 u_e c > 1$, which is the usual case. Eq. (14) sets an upper limit on transportable beam current density above which channel filamentation will develop.

4. CONCLUSIONS

The stability conditions in Eqs. (5), (13) and (14), identify important constraints on beam propagation. Eq. (5) together with Eq. (6) states that the plasma cannot be heated above a certain critical temperature without generating electrostatic microturbulence. Such turbulence will degrade beam quality and confinement. In general the most severe constraint on T_e exists at the tail of the beam before bunching occurs where the critical temperature is defined by

$$T_e^C(eV) \equiv 10^{-6}\left(\frac{\mu_b^2 n_p^3 z_p^5 \lambda_{ei}^2 \alpha_m^8}{z_b^4 n_b^2(z=0)}\right)^{1/3} , \qquad (15)$$

where n_p is given in Eq. (6). By increasing n_p the critical temperature can be raised at the expense of increasing the beam energy loss during transport. Operating at twice the density specified in Eq. (6) increases T_e^C by a factor of two but only increases the beam energy loss by 25%. The actual temperature that the electrons will reach for a given beam and background gas is not always easily estimated and must be calculated on a case to case basis and compared with the critical temperature defined in Eq. (15). Here α_m is a measure of the spread in axial velocities in the beam, which for a monoenergetic beam is given by $\Delta V_z/V_b \sim \alpha_m^2/2$. If the beam has a spread in energy such that $\alpha_m^2 < \Delta E/E$, then α_m^8 in Eq. (15) should be replaced by $(\Delta E/E)^4$.

Growth of electromagnetic waves can be held to a tolerable level by allowing for a reasonable spread in beam perpendicular energy and limiting the beam current density. If the beam is too cold, beam filamentation can occur during beam transport. The condition for good beam transport is given in Eq. (13). If the beam does not filament but the beam current density is too high, the return current in the channel can cause channel filamentation. In order to prevent this from occurring Eq. (14) should be satisfied. The conditions given in Eqs. (13) and (14) may actually be too severe since channel hydrodynamic effects have not been included self consistently in the analysis. Channel expansion due to $J \times B$ force may tend to prevent growth of these transverse modes. These effects are presently under investigation.

5. REFERENCES

1. S. A. Goldstein and R. Lee, Phys. Rev. Lett. 35, 1079 (1975).

2. J. W. Poukey, J. R. Freeman, M. J. Clauser, and G. Yonas, Phys. Rev. Lett. 35, 1806 (1975).

3. J. W. Poukey, J. Vac. Sci. Technol. 12, 1214 (1975)

4. A. E. Blaugrund, G. Cooperstein, J. R. Boller and S. A. Goldstein Bull. Am. Phys. Soc. 20, 1252 (1975).

5. P. A. Miller, C. W. Mendel, D. W. Swain, and S. A. Goldstein, in Proceedings of the International Topical Conference on Electron Beam Research and Technology, Albuquerque, New Mexico (1975), p. 619.

6. G. Cooperstein, S. J. Stephanakis, J. R. Boller, R. Lee, and S. A. Goldstein, in Proceedings of the 1976 IEEE International Conference on Plasma Science, Austin, Texas (IEEE, New York, 1976), p. 126.

7. D. J. Johnson. G. W. Kuswa, A. V. Farnsworth, Jr., J. P. Quintenz, R. J. Leeper, E. J. T. Burns, and S. Humphries, Jr., Phys. Rev. Lett. 42, 610 (1979); D. J. Johnson, Bull. Am. Phys. Soc. 24, 925 (1979).

8. G. Cooperstein, S. A. Goldstein, D. Mosher, W. F. Oliphant, F. L. Sandel, S. J. Stephanakis and F. C. Young in Proceedings Third International Topical Conference on High Power Electron and Ion Beam Research and Technology, Novosibirsk, USSR (1979).

9. G. Cooperstein, S. A. Goldstein, D. Mosher, R. J. Barker, J. R. Boller, D. G. Colombant, A. Drobot, R. A. Meger, W. F. Oliphant, P. F. Ottinger, F. L. Sandel, S. J. Stephanakis and F. C. Young, in Laser Interaction and Related Plasma Phenomena, edited by H. Schwarz, H. Hora, M. Lubin and B. Yaakobi, (Plenum Press, New York, 1980).

10. R. O. Bangerter and D. J. Meeker, in Proceedings of the Second International Topical Conference on High Power Electron and Ion Beam Research and Technology, Ithaca, New York (1977), p. 183; J. H. Nuckolls, in Proceedings of the Topical Meeting on ICF (Opt. Soc. of Am. Wash., DC, 1978) paper TuA5.

11. S. A. Goldstein, D. P. Bacon, D. Mosher and G. Cooperstein Proceedings of the Second International Topical Conference on High Power Electron and Ion Beam Research and Technology, Ithaca, New York (1977), p. 71.

12. D. Mosher, G. Cooperstein, S. A. Goldstein, in Digest of the Topical Meeting on ICF (Opt. Soc. of Am., Wash., DC, 1980), paper ThC5.

13. D. Mosher, Bull. Am. Phys. Soc. 24, 926 (1979).

14. D. Mosher and S. A. Goldstein, Bull. Am. Phys. Soc. 23, 800 (1978).

15. D. G. Colombant, D. Mosher and S. A. Goldstein, Phys. Rev. Lett. 45, 1253 (1980).

16. P. F. Ottinger, D. Mosher and S. A. Goldstein, Phys. Fluids 23, 909 (1980).

17. P. F. Ottinger, D. Mosher and S. A. Goldstein, Phys. Fluids 22, 332 (1979).

18. P. F. Ottinger, D. Mosher and S. A. Goldstein, Phys. Fluids 24, 164 (1981).

19. F. Sandel. G. Cooperstein, S. A. Goldstein, D. Mosher and S. J. Stephanakis, Bull. Am. Phys. Soc. 24, 1031 (1979).

20. D. A. Hammer and N. Rostoker, Phys. Fluids 13, 1831 (1970).

21. B. S. Newberger and L. E. Thode, Bull. Am. Phys. Soc. 24, 1097 (1979).

22. P. F. Ottinger, Conference Record-Abstracts of the 1980 IEEE International Conference on Plasma Science, Madison, Wisconsin (IEEE, New York, 1980), p. 57.

23. V. U. Abramovich and V. I. Sevchenko. JETP 35, 730 (1972).

24. P. F. Ottinger, S. A. Goldstein and D. Mosher, NRL Memorandum Report 4180 (1980).
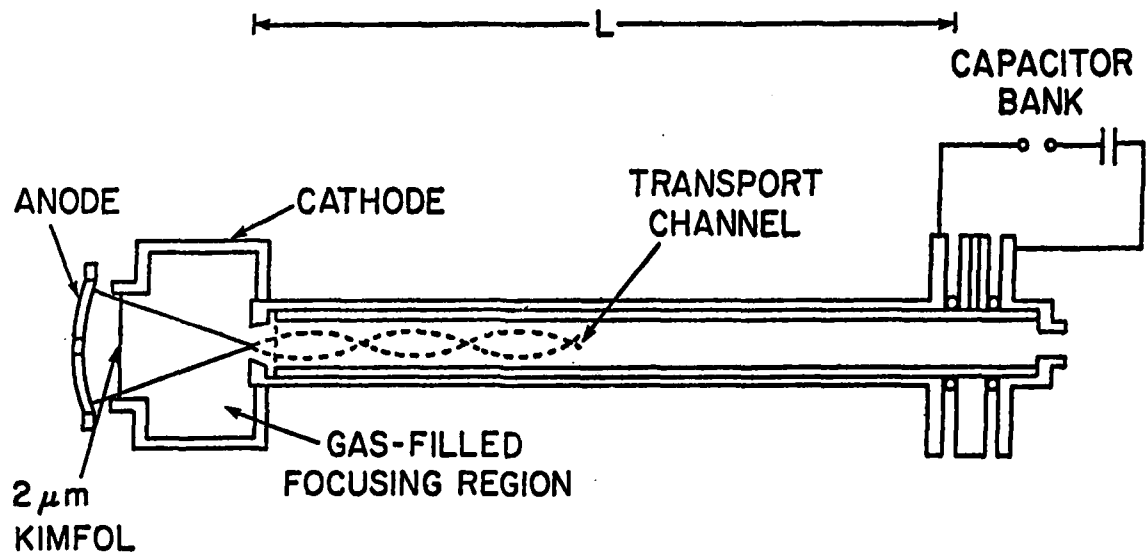
IDEAL DIODE VOLTAGE WAVEFORM:

$$\phi(t) = \frac{\phi_0}{(1 - t/t_a)^2} \quad ; \quad 0 \leq t \leq \tau_b < t_a$$

Fig. 1—Schematic of ion diode, focusing region and transport channel for light ion beam ICF module. The ideal diode voltage waveform for axial bunching is also shown where ϕ_0 in the initial diode voltage, t_a is the beam arrival time at the target and $\bar{\tau}_b$ is the beam pulse duration at injection.
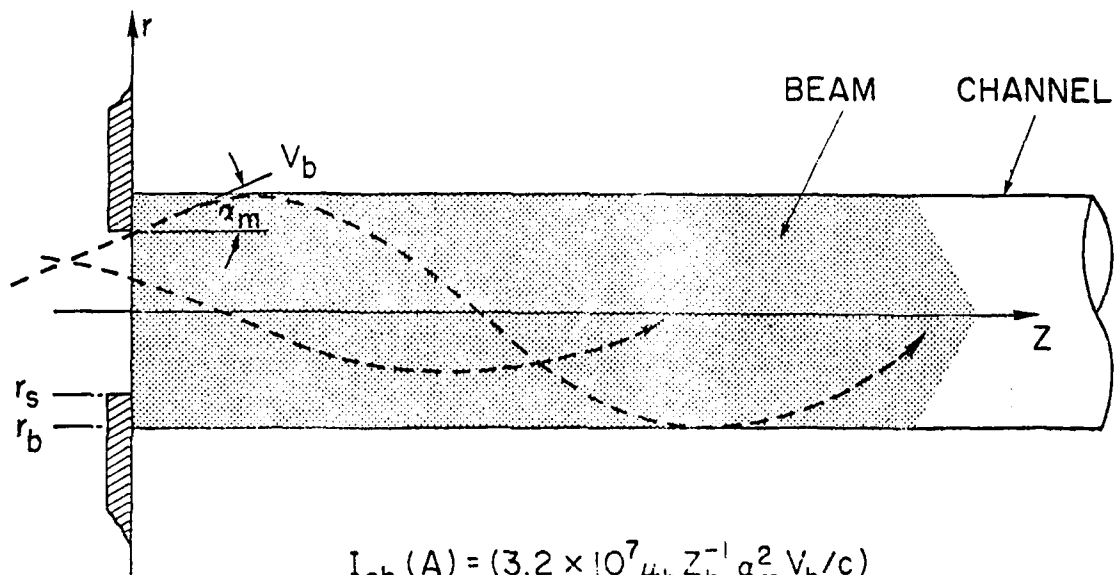
$$I_{ch}(A) = (3.2 \times 10^7 \mu_b Z_b^{-1} \alpha_m^2 V_b/c)$$

Fig. 2—Schematic of beam propagation in a z-discharge channel. Here $\frac{1}{2}m_i V_b = Z_d e \phi$ (where Z_d is beam ion charge state in the diode and ϕ is the diode voltage), α_m is the maximum injection angle, r_s is the beam spot size (or aperture size) and r_b is the beam radius in the channel. Also shown is the channel current required to confine the beam where Z_b is the charge state of the beam ions in the channel and $\mu_b = m_b/m_H$.
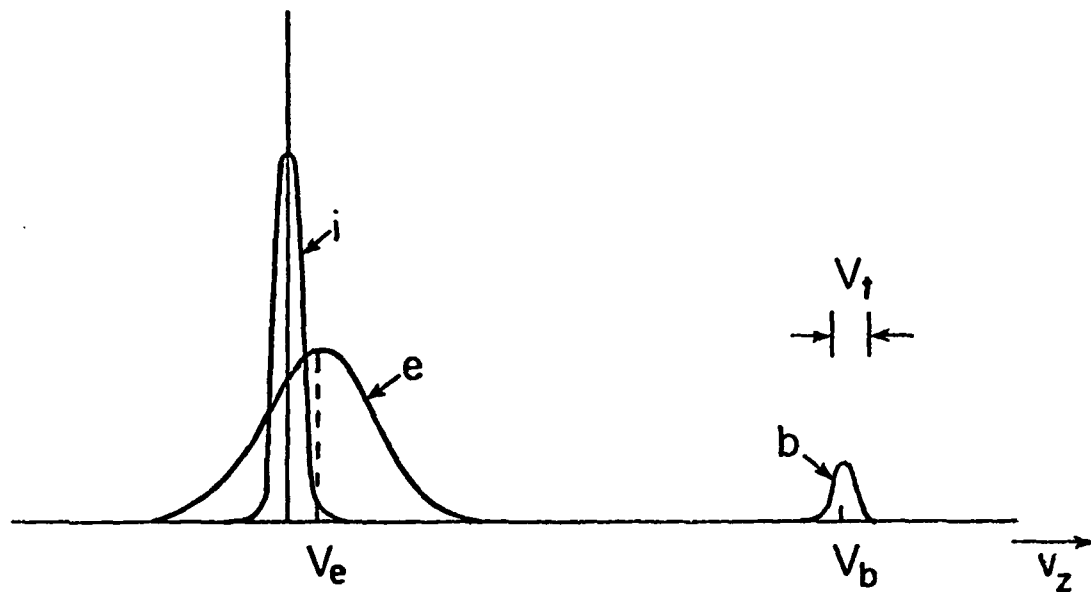
$$T_e \gtrsim T_i$$

$$\nu_{ei}(T_e) > \omega_{ce}$$

$$V_e \approx Z_b n_b V_b / Z_p n_p < \left(T_e/m_e\right)^{1/2}$$

BEAM:

$$V_b/c << 1$$

$$n_b << n_p$$

$$\frac{V_t}{V_b} \approx a_m^2$$

Fig. 3—Schematic of particle distribution in v_z. Here i, e and b are the plasma ions, plasma electrons and beam ions, respectively, and V_t is the measure of the spread in the beam distribution. Other typical beam-plasma conditions are also listed.

14

$$f_b = N \exp\left[-\frac{(v_z - V_b)^2}{V_t^2}\right]$$

(A)

O $\quad V_b \quad$ v_z

$$f_b = N\left[H(v_z - V_b + V_t) - H(v_z - V_b - V_t)\right]$$

(B)

O $\quad V_b - V_t \quad V_b + V_t \quad$ v_z

(C)

O $\quad V_b \quad$ v_z
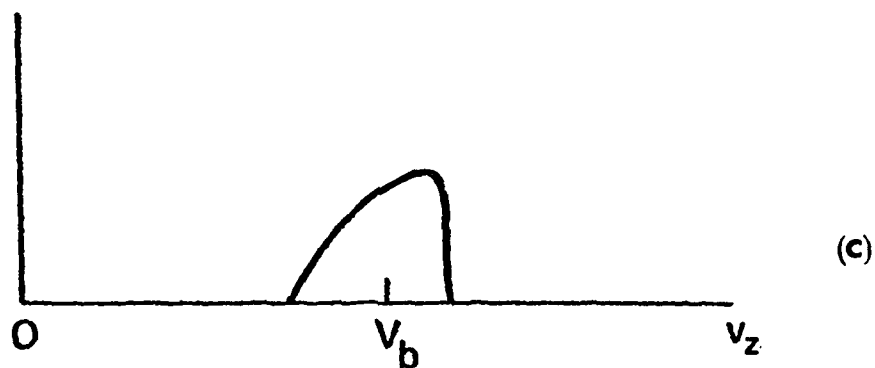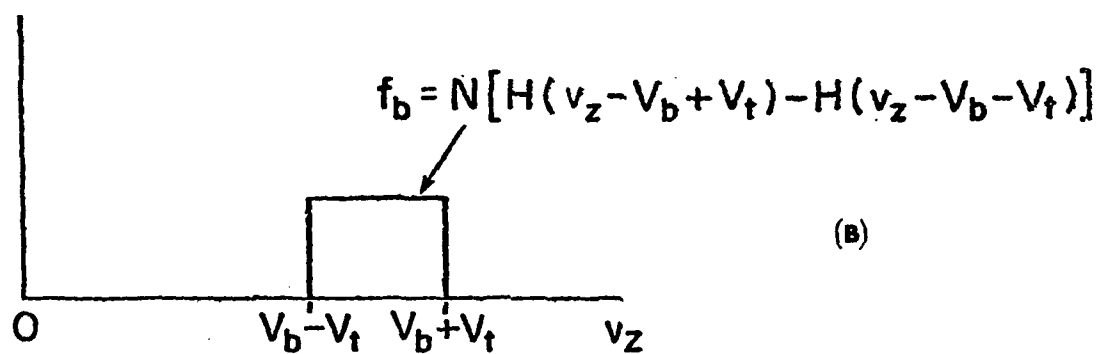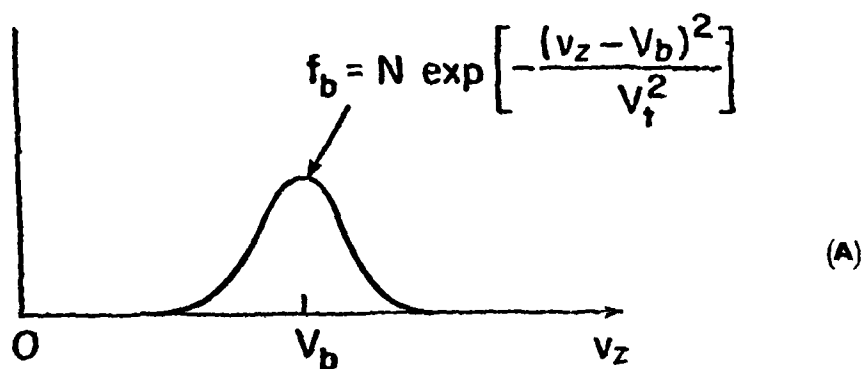
Fig. 4--Distribution of beam ions in v_z for (a) a uniform distribution, (b) a Gaussian distribution actual distribution and (c)

15

$$Z = \overline{V}_z t + \Delta Z \sin 2 \omega_\beta t$$
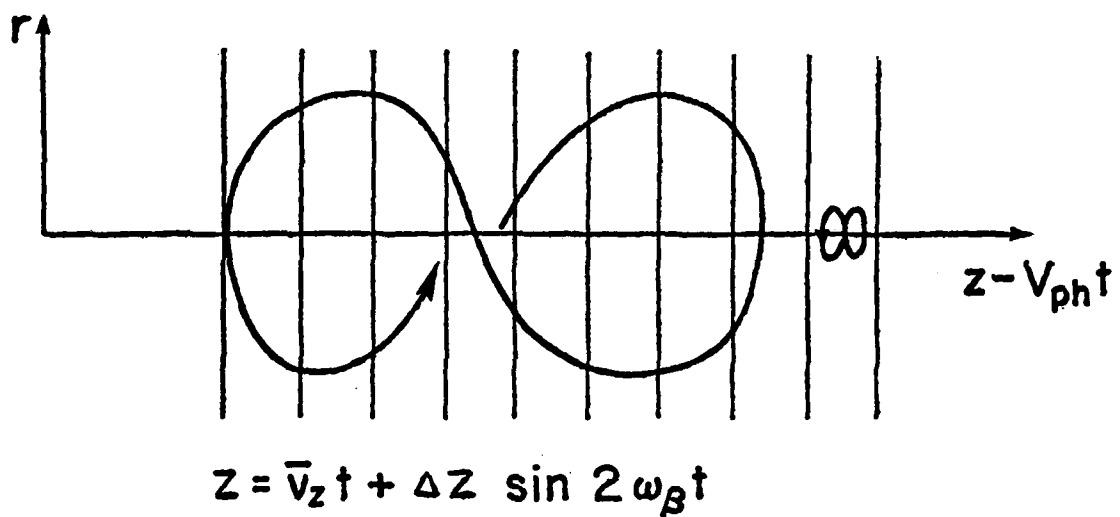
Fig. 5—Beam ion orbits in a frame of reference moving with the phase velocity of an ES wave
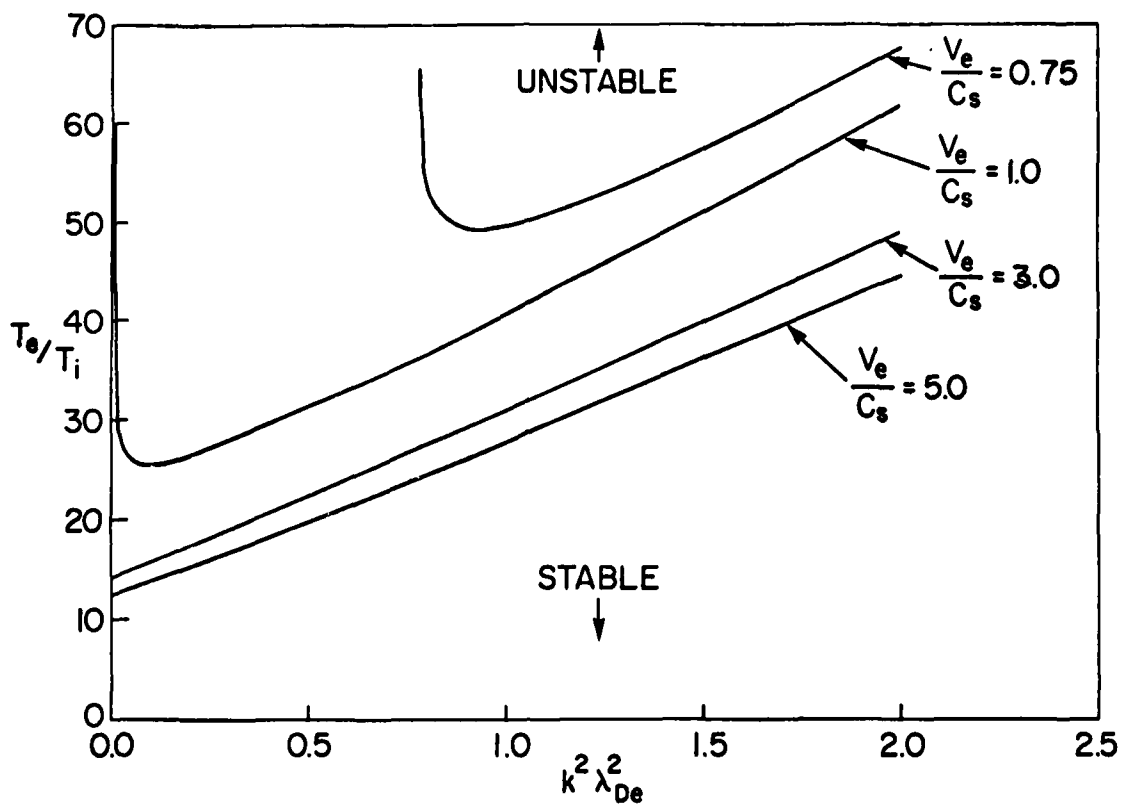
Fig. 6—Critical values of T_e/T_i for ion-acoustic instability (assuming $\nu_{ei} = 0$). Regions above the curves are unstable and below the curves are stable.

17

19

AF Weapons Laboratory, AFSC
Kirtland AFB, NM 87117

Attn:	CA	1 copy
	ELC	1 copy
	NT	1 copy
	SUL	1 copy
	DYP	1 copy
	J. Darrah	1 copy
	W.L. Baker	1 copy

HQ USAF/SD
Washington, DC 2033.

| Attn: RDQSM | 1 copy |

Director
Joint Strat Tgt Planning Staff JCS
OFFUTT AFB
Omaha, NE 68113

| Attn: JSAS | 1 copy |

SAMSO/DY
Post Office Box 92960
Worldway Postal Center
Los Angeles, CA 90009
(Technology)

| Attn: DS | 1 copy |

SAMSO/IN
Post Office Box 92960
Worldway Postal Center
Los Angeles, CA 90009

| Attn: IND MAJ D. S. Muskin | 1 copy |

SAMSO/MN
Norton AFB, CA 92409
(Minuteman)

| Attn: MNNH | 1 copy |

SAMSO/SK
Post Office Box 92960
Worldway Postal Center
Los Angeles, CA 90009
(Space Comm Systems)

| Attn: SKF P. H. Stadler | 1 copy |

U. S. Department of Energy
Division of Inertial Fusion
Washington, DC 20545

Attn:	G. Canavan	1 copy
	T. F. Godlove	1 copy
	S. L. Kahalas	1 copy
	R. L. Schriever	1 copy

Argonne National Laboratory
9700 South Cass Avenue
Argonne, Illinois 60439

| Attn: | G. R. Magelssen | 1 copy |
| | R. J. Martin | 1 copy |

Brookhaven National Laboratory
Upton, NY 11973

| Attn: A. F. Maschke | 1 copy |

Lawrence Berkley Laboratory
Berkeley, CA 94720

| Attn: D. Keefe | 1 copy |

Lawrence Livermore National Laboratory
P. O. Box 808
Livermore, CA 94550

Attn:	L-18	1 copy
	L-153	1 copy
	R. O. Bangerter	1 copy
	R. J. Briggs	1 copy
	E. P. Lee	1 copy
	J. H. Nuckolls	1 copy
	S. S. Yu	1 copy
	Tech Info Dept. L-3	1 copy

Los Alamos National Laboratory
P. O. Box 1663
Los Alamos, NM 87545

Attn:	B. B. Henderson	1 copy
	K. B. Perkins	1 copy
	L. E. Thode	1 copy

National Science Foundation
Mail Stop 19
Washington, DC 20550

| Attn: D. Berley | 1 copy |

Sandia National Laboratories
P. O. Box 5800
Albuquerque, NM 87115

Attn:	J. R. Freeman	1 copy
	S. Humphries	1 copy
	D. J. Johnson	1 copy
	G. W. Kuswa	1 copy
	P. S. Miller	1 copy
	J. P. Vandevender	1 copy
	G. Yonas	1 copy
	Doc Con for 3141 Sandia RPT Coll	1 copy

AVCO Research and Systems Group
201 Lowell Street
Wilmington, MA 01887

| Attn: Research Lib. A830 Rm. 7201 | 1 copy |

BDM Corporation, The
795 Jones Branch Drive
McLean, VA 22101

| Attn: Tech Lib. | 1 copy |

Boeing Company, The
P. O. Box 3707
Seattle, WA 98124

| Attn: Aerospace Library | 1 copy |

Cornell University
Ithaca, NY 14850

Attn:	D. A. Hammer	1 copy
	R. N. Sudan	1 copy
	J. Maenchen	1 copy

Dikewood Industries, Inc.
1009 Bradbury Drive, SE
Albuquerque, NM 87106

| Attn: L. W. Davis | 1 copy |

EG&G, Inc.
Albuquerque Division
P. O. Box 10218
Albuquerque, NM 87114

| Attn: Technical Library | 1 copy |

20

Ford Aerospace & Communications Operations
Ford & Jamboree Roads
Newport Beach, CA 92663
(Formerly Aeronutronic Ford Corporation)

Attn: Tech Info Section   1 copy

Ford Aerospace & Communications Corp
3939 Fabian Way
Palo Alto, CA 94303
(Formerly Aeronutronic Ford Corporation)

Attn: Library   1 copy
      D. R. McMorrow MS G 30   1 copy

General Electric Company
Space Division
Valley Forge Space Center
Goddard Blvd., King of Prussia
P. O. Box 8555
Philadelphia, PA 19101

Attn: J. C. Peden VFSC, Rm. 4230M   1 copy

General Electric Company
Tempo-Center for Advanced Studies
816 State Street (P. O. Drawer QQ)
Santa Barbara, CA 93102

Attn: DASIAC   1 copy.

Grumman Aerospace Corporation
Bethpage, NY 11714

Attn: P. Suh   1 copy

Institute for Defense Analyses
400 Army-Navy Drive
Arlington, VA 22202

Attn: IDA Librarian R. S. Smith   1 copy

Ion Physics Corporation
South Bedford Street
Burlington, MA 01803

Attn: H. Milde   1 copy

IRT Corporation
P. O. Box 81087
San Diego, CA 92138

Attn: R. L. Mertz   1 copy

JAYCOR, Inc.
205 S. Whiting Street
Alexandria, VA 22304

Attn: J. Guillory   1 copy
      R. Hubbard   1 copy
      R. Sullivan   1 copy
      D. A. Tidman   1 copy

JAYCOR, Inc.
1401 Camino Del Mar
Del Mar, CA 92014

Attn: E. Wenaas   1 copy

JAYCOR, Inc.
300 Unicorn Park Drive
Woburn, MA 01801

Attn: H. Linnerud   1 copy

Kaman Science Corporation
P. O. Box 7463
Colorado Springs, CO 80933

Attn: A. P. Bridges   1 copy
      D. H. Bryce   1 copy
      J. R. Hoffman   1 copy
      W. E. Ware   1 copy

Lockheed Missiles and Space Co., Inc.
3251 Hanover Street
Palo Alto, CA 94304

Attn: L. F. Chase   1 copy

Massachusetts Institute of Technology
Cambridge, MA 02139

Attn: R.C. Davidson   1 copy
      G. Bekefi   1 copy
      D. Hinshelwood   1 copy

Maxwell Laboratories, Inc.
9244 Balboa Avenue
San Diego, CA 92123

Attn: R. W. Clark   1 copy
      A. C. Kolb   1 copy
      P. Korn   1 copy
      A. R. Miller   1 copy
      J. Pearlman   1 copy

McDonnell Douglas Corporation
5301 Bolsa Avenue
Huntington Beach, CA 92647

Attn: S. Schneider   1 copy

Mission Research Corporation
1400 San Mateo Blvd. SE
Albuquerque, NM 87108

Attn: B. B. Godfrey   1 copy

Mission Research Corporation-San Diego
P. O. Box 1209
LaJolla, CA 92038

Attn: V.A.J. Van Lint   1 copy

Mission Research Corporation
735 State Street
Santa Barbara, CA 93101

Attn: W. C. Hart   1 copy
      C. L. Longmire   1 copy

Northrop Corporation
Electronic Division
2301 West 120th Street
Hawthorne, CA 90250

Attn: V. R. DeMartino   1 copy

Northrop Corporation
Northrop Research and Technology Ctr.
3401 West Broadway
Hawthorne, CA 90205   1 copy

Physical Dynamics
P.O. Box 556
La Jolla, CA 92037

Attn: S. Jorna   1 copy

Physics International Co.
2700 Merced Street
San Leandro, CA 94577

Attn: J. Benford   1 copy
B. Bernstein   1 copy
G. Frazier   1 copy
R. Genuario   1 copy
E. B. Goldman   1 copy
R. Huff   1 copy
A. J. Toepfer   1 copy

Pulsar Associates, Inc.
11491 Sorrento Valley Blvd.
San Deigo, CA 92121

Attn: C. H. Jones, Jr.   1 copy

Princeton Plasma Physics Laboratory
James Forrestal Campus
P.O. Box 451
Princeton, N.J. 08540

Attn: R. Kulsrud   1 copy

Pulse Sciences, Inc.
1615 Broadway, Suite 610
Oakland, CA 94612

Attn: I. Smith   1 copy
P. Spence   1 copy
S. Putman   1 copy

R&D Associates
P. O. Box 9695
Marina Del Rey, CA 90291

Attn: W. R. Graham, Jr. 1 copy
H. Grover   1 copy
C. MacDonald   1 copy
E. Martinelli   1 copy

R&D Associates
Suite 500
1401 Wilson Blvd.
Arlington, VA 22209

Attn: P. J. Turchi   1 copy

Science Applications, Inc.
P. O. Box 2351
LaJolla, CA 92038

Attn: J. Robert Beyster 1 copy

Spire Corporation
P. O. Box D
Bedford, MA 01730

Attn: R. G. Little   1 copy

SRI International
333 Ravenswood Avenue
Menlo Park, CA 94025

Attn: Setsuo Ddairiki   1 copy

Stanford University
SLAC
P. O. Box 4349
Stanford, CA 94305

Attn: W. B. Herrmannsfeldt 1 copy

Systems, Science and Software, Inc.
P. O. Box 1620
LaJolla, CA 92038

Attn: A. R. Wilson   1 copy

Texas Tech University
P. O. Box 5404 North College Station
Lubhock, TX 79417

Attn: T. L. Simpson   1 copy

TRW Defense and Space Sys Group
One Space Park
Redondo Beach, CA 90278

Attn: Tech Info Center/S-1930 1 copy
Z.G.T. Guiragossian   1 copy
D. Arnush   1 copy

University of California
Dept. of Physics
La Jolla, CA 92037

Attn: K. Brueckner   1 copy
W.B. Thompson   1 copy

University of California
Boelter Hall 7731
Los Angeles, CA 90024

Attn: F.F. Chen   1 copy

University of California
Irvine, CA 90024

Attn: G. Benford   1 copy
N. Rostoker   1 copy

University of Illinois
Urbana, IL 61301

Attn: G. H. Miley   1 copy
J. T. Verdeyen   1 copy

University of Rochester
Laboratory of Laser Energetics
River Station, Hopeman 110
Rochester, NY 14627

Attn: M. J. Lubin   1 copy

University of Scranton
Dept. of Physics
Scranton, PA 18510

Attn: E. Murray   1 copy

U. S. Department of Energy
P. O. Box 62
Oak Ridge, TN 37830   50 copies

Vought Corporation
Michigan Division
38111 Van Dyke Road
Sterling Heights, MI 48077
(Formerly LTV Aerospace Corp)

Attn: Tech Lib   1 copy

Atomic Weapons Research Establishment
Building H3
Aldermaston, Reading RG 7 4PR
United Kingdom

Attn: J. C. Martin   1 copy

22

DATE
ILMED
—8